S_N1 Dissociation Pathways for *N*-Benzylpyridiniums. A Search Using Molecular Orbital Methods for Ion–Molecule Complexes as Possible Reaction Intermediates[1,§]

Alan R. Katritzky* and Nageshwar Malhotra

Department of Chemistry, University of Florida, Gainesville, Florida 32611-2046

George P. Ford

Department of Chemistry, Southern Methodist University, Dallas, Texas 75275

Ernst Anders* and Jurgen G. Tropsch

Institut für Organische Chemie der Universitaet, Erlangen-Nuernberg, Henkestrasse 42, D-8520 Erlangen, Germany

Received September 4, 1990 (Revised Manuscript Received April 30, 1991)

Semiempirical MO calculations (AM1, MNDO, and PM3) predict that unimolecular dissociation of *N*-benzylpyridiniums leads initially to ion–molecule complexes, which in some cases are of significantly lower energy than the fully dissociated products. The calculations support an earlier suggestion of the existence of such intermediates made on the basis of experimentally determined activation volumes and of the behavior of some of these cations toward nucleophilic reagents.

Mechanisms of nucleophilic substitution at saturated carbon atoms have been greatly clarified by the use of pyridines as neutral leaving groups.[2] Whereas unimolecular mechanisms for anionic leaving groups are restricted to high dielectric constant media because of charge creation in the transition state, unimolecular dissociations of the type $RPy^+ \rightarrow R^+ + Py$ can be studied in solvents of low dielectric constant and in the gas phase. Earlier work in one of our groups established a wide spectrum of mechanisms for nucleophilic displacement of the N-substituent from N-substituted pyridines.[2] For example, the rates of benzylation of piperidine by the crowded N-substituted pyridinium cations 1 and of 4-methoxybenzylation of piperidine by the 7-phenyl derivative of 2 both follow second-order kinetics in chlorobenzene at normal pressure.[3] Raising the pressure was expected to increase these rates, since the reactions were expected to exhibit negative activation volumes ($\Delta V^{\ddagger}$), typical of those involving bimolecular transition states.[4] In contrast, as the pressure was increased to 55 MPa, both rates were found to gradually decrease.[5] This was tentatively explained in terms of a kinetic scheme in which the highly hindered *N*-benzylpyridinium, $^+PyCH_2Ph$, is in equilibrium with an ion–molecule complex [$Py\cdots{}^+CH_2Ph$], which then reacts irreversibly with the unhindered nucleophile Nu (Scheme I).

Similar ion–molecule complex intermediates are also present in the gas phase. Thus, we have shown[6] that *N*-alkylpyridinium ions can yield rearranged alkylcarbonium ions, under these conditions, and that such rearrangements can occur while there is still considerable bonding between the pyridine nitrogen and the carbon atom carrying a partial positive charge.

We now report the results of molecular orbital calculations using the AM1[7] method, which were undertaken to seek theoretical support for the existence of such ion–molecule complexes (I–MC) as discrete entities. We also did some work with the MNDO[8] and PM3[9] methods. Specifically, reaction pathways were calculated for the S_N1 dissociations (Scheme I) for nine compounds (Chart I, 1–9) using the distance between the benzyl carbon and the pyridine nitrogen atom as the reaction coordinate. Structures 1–9 were chosen to reflect synthetically accessible pyridinium compounds for which kinetic, X-ray crystallographic, and/or mass spectral data were available.

Scheme I. Reaction Coordinates for Dissociation

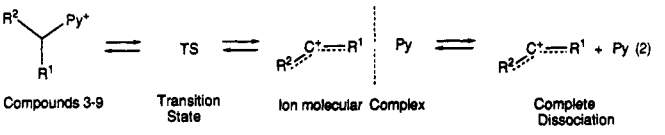

Py: Pyridine or a substituted pyridine

Chart I. Pyridinium Cations Treated Theoretically[a]

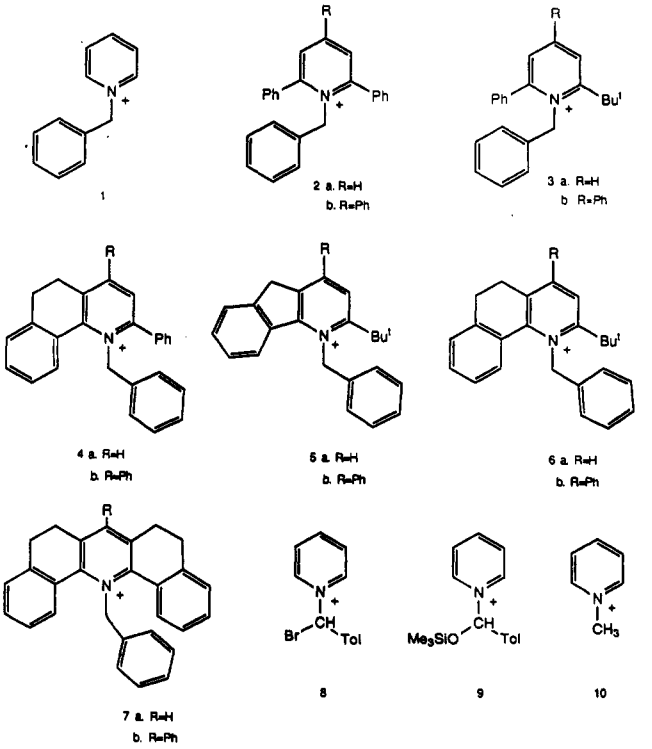

[a] For 2–7, the a compounds we calculated, but comparisons were made with properties of the b compounds.

† This paper is dedicated to Prof. H. J. Bestmann on the occasion of his 65th birthday (E.A. and A.R.K.).

0022-3263/91/1956-5039$02.50/0

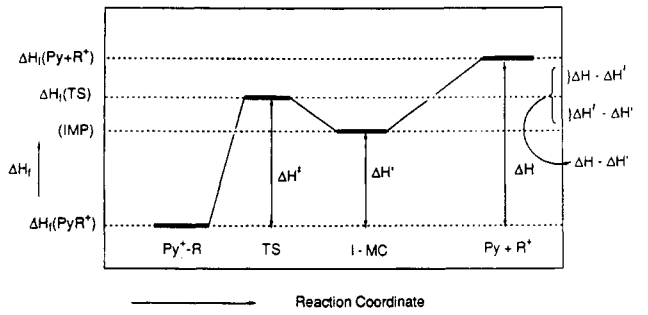

Figure 1. Definitions of enthalpies of formation of different species along reaction coordinate.

However, in our treatment of compounds **2–7**, the 4-phenyl substituents were omitted to simplify the calculations; i.e., the calculations were done on **2a–7a** but comparisons were made with the experimental data of compounds **2b–7b**. Similarly, *p*-methyl (in **3b**) and *p*-chloro (in **5b**) substituents in the *N*-benzyl groups were omitted in the calculations.

Methods and Procedure

The enthalpies of formation of the species considered are defined in Figure 1: all are relative to the starting pyridinium cation as zero. Thus, $\Delta H^{\ddagger}$ refers to the transition state, $\Delta H'$ to the ion–molecule complex, and ΔH to the completely dissociated products. All calculations were carried out using Version 4 of the MOPAC package.[10,11] Geometries were completely optimized with the stopping criteria defined by the "PRECISE" option. (To avoid problems associated with incompletely converged geometries the key word PRECISE specifies more stringent stopping criteria for both the SCF procedure and the minimization algorithms than provided by the program defaults. The many stopping criteria involved and their specific values are well-documented in the MOPAC manual. This topic is discussed more fully in: Boyd, D. B.; Smith, D. W.; Stewart, J. J. P.; Wimmer, E. *J. Comput. Chem.* **1988**, *9*, 387.) In most cases, initial input geometries were generated using the MMX force field incorporated in PCMODEL.[12] As shown for **1**, **8**, and **9**, this MMX procedure facilitates the search for the most stable conformation.[13a] The lowest energy conformations for each of the ions **1–9** were used as the input data to MOPAC, and the most stable conformation thus found for each compound at the semiempirical level was used in subsequent studies. The dissociation pathways of **1–9** were followed by gradually extending the C–N bond length while minimizing the energy of the system with respect to all remaining geometrical variables. In most cases, the approximate transition states located

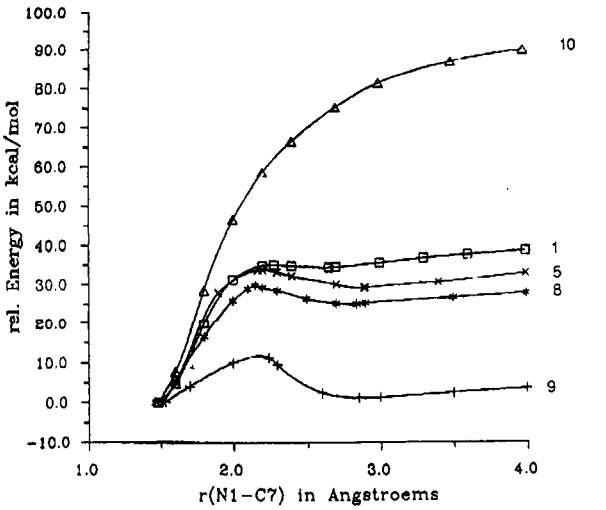

Figure 2. Summary of the AM1 results and energy profiles for the dissociation of substituted *N*-alkylpyridinium ions: **1** (□), **5** (×), **10** (△), **8** (*), **9** (+). As the curves of **2–4**, **6**, and **7** are similar to those of **1** and **5**, they are not included in this figure.

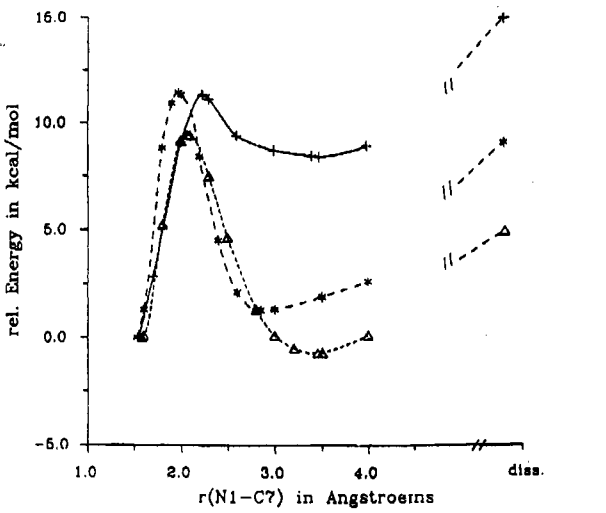

Figure 3. Energy profiles for the dissociation of **9** calculated using the AM1 (*), MNDO (△), and PM3 (+) methods.

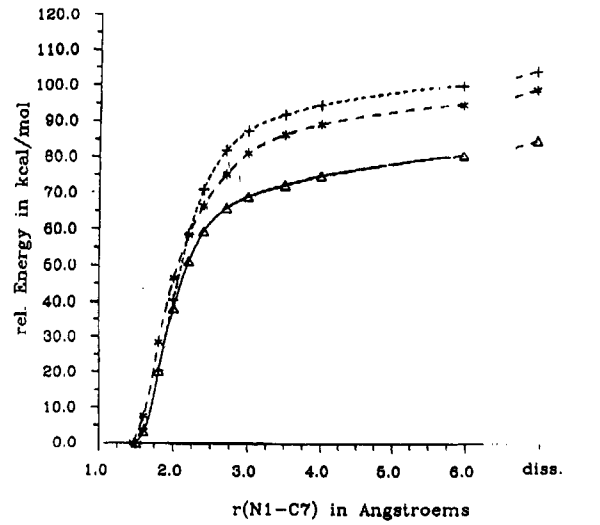

Figure 4. Energy profiles for the dissociation of 1-methylpyridinium cation **10** calculated using the AM1 (*), MNDO (△), and PM3 (+) methods.

(1) Kinetics and Mechanisms of Nucleophilic Displacement. 29. Part 28: Katritzky A. R.; Watson, C. H.; Dega-Szafran, Z.; Eyler, J. R. *J. Chem. Soc., Perkin Trans. 2* **1990**, 1051.

(2) For reviews, see: (a) Katritzky, A. R.; Sakizadeh, K.; Musumarra, G. *Heterocycles* **1985**, *23*, 1765. (b) Katritzky, A. R.; Musumarra, G. *Chem. Soc. Rev.* **1984**, *13*, 47. (c) Katritzky, A. R.; Brycki, B. E. *Chem. Soc. Rev.* **1990**, *19*, 83.

(3) Katritzky, A. R.; El-Mowafy, M.; Musumarra, G.; Sakizadeh, K.; Sana-Ullah, S. M.; El-Shafie, M.; Thind, S. S. *J. Org. Chem.* **1981**, *46*, 3823.

(4) Asano, T.; le Noble, W. J. *Chem. Rev.* **1978**, *78*, 407.

(5) Katritzky, A. R.; Sakizadeh, K.; Gabrielsen, B.; le Noble, W. J. *J. Am. Chem. Soc.* **1984**, *106*, 1879.

(6) Katritzky, A. R.; Watson, C. H.; Dega-Szafran, Z.; Eyler, J. R. *J. Am. Chem. Soc.* **1990**, *112*, 2471.

(7) Dewar, M. J. S.; Zoebisch, E. G.; Healy, E. F.; Stewart, J. J. P. *J. Am. Chem. Soc.* **1985**, *107*, 3902. Dewar, M. J. S.; Jie, C. *Organometallics* **1987**, *6*, 1486. Dewar, M. J. S.; Zoebisch, E. G. *THEOCHEM* **1988**, *180*, 1.

(8) (a) Dewar, M. J. S.; Thiel, W. *J. Am. Chem. Soc.* **1977**, *99*, 4899. (b) Dewar, M. J. S.; Thiel, W. *Ibid.* **1977**, *99*, 4907. (c) Dwar, M. J. S.; Healy, E. *J. Comput. Chem.* **1983**, *4*, 542.

(9) (a) Stewart, J. J. P. *J. Comput. Chem.* **1989**, *10*, 209. (b) Stewart, J. P. P. *Ibid.* **1989**, *10*, 221.

(10) Stewart, J. J. P. *QCPE* **1989**, *9*, 10.

(11) Calculations at SMU were carried out on a local adaption of this package for the Harris H800 series of minicomputers: Ford, G. P. *QCPE* **1989**, *9*, 53.

(12) Serena Software, Box 3076, Bloomington, IN.

(13) (a) Anders, E.; Irmmer, E.; Sheldrick, G. M. *Chem. Ber.* **1990**, *123*, 321. (b) Chandrasekar, J.; Budzelaar, P. H. M.; Clark, T. Unpublished work.

Table I[a,b]

struct	ΔH_f(PyR$^+$)	ΔH_f(TS)	ΔH_f(I-MC)	ΔH_f(Py)	r(PyR$^+$)	r(TS)	r(I-MC)
1	210.1	245.4	244.8	32.0	1.476	2.282	2.628
2	263.2	297.1	295.9	87.3	1.469	2.245	2.668
3	226.1	257.9	253.0	42.1	1.469	2.161	2.905
4	255.4	292.0	288.2	79.2	1.470	2.169	2.774
5	230.3	264.9	260.2	47.6	1.469	2.173	2.882
6	219.1	253.6	244.3	32.4	1.468	2.075	2.932
7	248.9	280.9	277.7	68.0	1.477	2.178	2.767
8	215.1	245.0	240.3	32.0	1.480	2.149	2.836
9	103.5	114.9	105.5	32.0	1.526	1.969	2.850
10	186.1	*c*	*c*	32.0	1.456	*c*	*c*

[a] Units: energies, kcal mol^{-1}; distances, Å; 4.184 kJ mol^{-1} = 1 kcal mol^{-1}. [b] For definition of ΔH_f quantities, see Figure 1. The r values denote C–N bond lengths in the cation, transition state, and ion–molecule complex as indicated. [c] Energies rises monotonically to dissociated products.

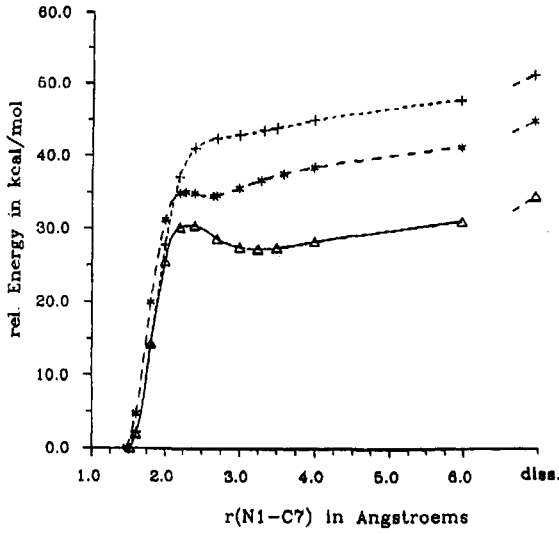

Figure 5. Energy profiles for the dissociation of 1 calculated using the AM1 (*), MNDO (△), and PM3 (+) methods.

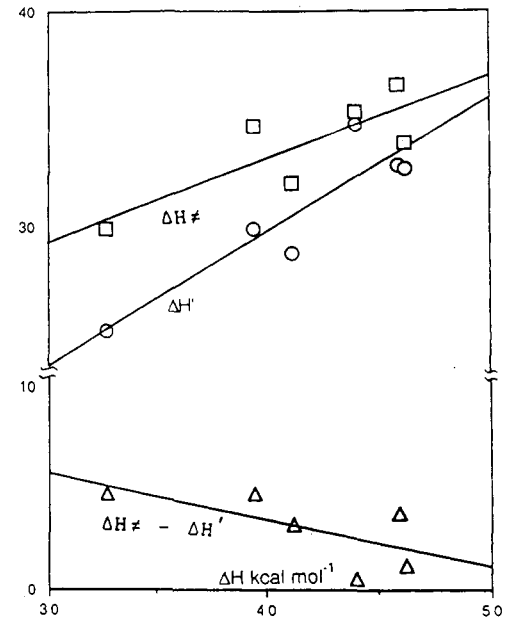

Figure 6. Relationship between ΔH and $\Delta H'$, $\Delta H^{\ddagger}$, and $\Delta H^{\ddagger} - \Delta H'$ (AM1). Data point from left to right: **5**, **4**, **7**, **8**, **2**, and **1**.

in this manner were refined using the local (Erlangen) implementation[13b] of Powell's[14] NS01A subroutine, rather than the default optimizer in the standard version of MOPAC. In each case diagonalization of the Cartesian force constant matrix revealed the required single negative eigenvalue characteristic of a genuine transition state (saddle point).[15]

Results and Discussion

Dissociation Pathways. The overall forms of the potential energy surfaces for C–N bond heterolysis are shown in Figure 2 for the representative cases **1**, **5**, and **8–10** at the AM1 level. The complete data are summarized in Tables I and V. For the less endothermic processes, calculations[16] clearly predict the presence of a broad potential minima lying below the energies of the fully dissociated products. As the reactions become progressively less endothermic the activation barriers ($\Delta H^{\ddagger} - \Delta H'$) that separate them from the covalently bound pyridinium ions become progressively smaller. For the highly endothermic loss of the methyl cation (from **10**) there is no discrete I–MC and thus no activation barrier separating this from the starting cation.

For all except compound **1**, the AM1, MNDO, and PM3 methods led in each case to a qualitatively similar reaction profile. A typical case is illustrated for the dissociation of **9** in Figure 3. For the methyl (nonbenzylic) ion **10** all the methods predict the dissociation to take place via a simple monotonic rise in energy (Figure 4). The dissociation of **1** (Figure 5) represents an intermediate situation revealing a shallow minimum at the AM1 level that is more pronounced in the MNDO calculation but disappears altogether at the PM3 level.

The qualitative form of the reaction profile for dissociation thus appears to be dominated by the overall energetics, as predicted by the Hammond postulate.[16] Indeed, there are rough quantitative correlations between ΔH and the corresponding relative enthalpies of the intermediate ($\Delta H'$) and the activation barriers to its formation ($\Delta H^{\ddagger}$) and an analogous inverse relationship with the barrier hindering return of the intermediate to the pyridinium ion ($\Delta H^{\ddagger} - \Delta H'$). These are shown for the AM1 results in Figure 6, and similar trends are evident for the MNDO and PM3 results. However, **9** falls outside the range of these correlations: the already low barrier to formation of the very stable intermediate is even lower than implied by the trend defined by the remaining data.

Intermediate Ion–Molecule Complex. The energy minima evident in Figures 2, 4, and 5 correspond to loose electrostatically bound ion–molecule complexes. The positive charge in these I–MC is almost completely localized on the carbonium ion moieties, with the calculated charge on the pyridine moiety not exceeding 0.025, and mostly much less. These species are therefore not charge-transfer complexes, nor is there any significant covalent bonding between the component moieties. We

(14) Powell, M. J. D. *Harwell Subroutine Library*; Theoretical Physics Division: Atomic Energy Research Establishment, Harwell, U.K., 1968.
(15) McIver, J. W., Jr.; Komornicki, A. *Chem. Phys. Lett.* **1971**, *10*, 303.
(16) Dewar, M. J. S.; Dougherty, R. C. *The PMO Theory of Organic Chemistry*; Plenum Press: New York, 1975, p 212. Hammond, G. S. *J. Am. Chem. Soc.* **1955**, *77*, 334.

Table II. MNDO Data for the Dissociation of Pyridinium Ions[a,b]

struct	ΔH_f(PyR$^+$)	ΔH_f(TS)	ΔH_f(I-MC)	ΔH_f(Py)	r(PyR$^+$)	r(TS)	r(I-MC)
1	212.4	243.7	240.4	28.7	1.518	2.317	3.250
2	264.7	296.4	287.2	76.7	1.515	2.245	2.574
4	263.6	292.6	279.3	67.0	1.512	2.167	3.863
5	247.1	273.8	257.3	43.4	1.511	2.167	4.294
7	253.6	281.5	270.2	57.8	1.518	2.204	3.740
8	216.3	245.3	238.5	28.7	1.514	2.228	3.315
9	92.7	12.0	91.9	28.7	1.577	2.071	3.450
10	188.6	*c*	*c*	28.7	1.500	*c*	*c*

[a] Units: energies, kcal mol^{-1}; distances, Å; 4.184 kJ mol^{-1} = 1 kcal mol^{-1}. [b] For definition of ΔH_f quantities, see Figure 1. The r values denote C-N bond lengths in the cation, transition state, and ion-molecule complex as indicated. [c] Energies rises monotonically to dissociated products.

Table III. PM3 Data for the Dissociation of Pyridinium Ions[a,b]

struct	ΔH_f(PyR$^+$)	ΔH_f(TS)	ΔH_f(I-MC)	ΔH_f(Py)	r(PyR$^+$)	r(TS)	r(I-MC)
1	207.5	*c*	*c*	30.4	1.502	*c*	*c*
8	206.2	249.7	*d*	30.4	1.495	2.737	*d*
9	85.3	96.6	93.7	30.4	1.550	2.237	3.486
10	183.5	*c*	*c*	30.4	1.481	*c*	*c*

[a] Units: energies, kcal mol^{-1}; distances, Å; 4.184 kJ mol^{-1} = 1 kcal mol^{-1}. [b] For definition of ΔH_f quantities, see Figure 1. The r values denote C-N bond lengths in the cation, transition state, and ion-molecule complex as indicated. [c] Energies rises monotonically to dissociated products. [d] The ion-molecule complex in this case collapses without activation to a hydrogen-bonded complex 36.7 kcal mol^{-1} higher in energy than 8 in which the distance between the nitrogen and α-hydrogen of benzyl moiety is 1.734 Å and the C-N distance 2.883 Å.

found that the energies of the free bases of 1, 2, 4, and 7 at their equilibrium geometries are less than 2 kcal mol^{-1} lower in energy then at the geometries found in the I-M complexes. This indicates only minor distortion in the I-M complexes. A typical example (that for 7) is shown in Figure 7: the benzyl moiety is stacked "above" the base at an angle of around 50° and separated by 2.76 ± 0.13 Å (AM1).

The above discussion refers to the gas phase and is thus immediately relevant to the appearance potentials for the unimolecular decomposition of N-substituted pyridiniums studied by ion-cyclotron resonance, which offers strong evidence for rearrangement in an intermediate ion-molecular complex.

$$PBz^+ \underset{k_{-1}}{\overset{k_1}{\rightleftharpoons}} P \qquad Bz^+ \xrightarrow{k_2[Nu]} Nu\text{-}Bz^+ + P \qquad (1)$$

We have already proposed the existence of ion-molecule complexes in solution to explain the kinetic and pressure dependence data in the benzylation and 4-methoxybenzylation of nucleophiles by the hindered pyridiniums **7b** and the 4-methoxybenzyl analogue of **2**.[5] Provided that $k_{-1} \gg k_2$[Nu] (eq 1), the overall reaction will show second-order kinetics with $k_{obs} \approx Kk_2$[PBz$^+$][Nu], where K is the equilibrium constant for the formation of I-MC from the starting pyridinium cation. The observed pressure dependence of k_{obs} will be the result of its opposing effects on K and k_2. Increase in pressures should decrease K and increase k_2. Since the measured activation volumes are positive,[5] the observed pressure dependence of k_{obs} is evidently dominated by variations in K, rather than k_2.

Just as for $\Delta V^{\ddagger}$, $\Delta S^{\ddagger}$ should also be a composite of opposing contributions associated with K and k_2. Activation entropies for bimolecular reactions are typically large and negative due to the dominant effect of the loss of rotational and translational degrees of freedom. The entropy ΔS for the equilibrium component should be positive and quite small since there is no change in the number of degrees of freedom. We have confirmed this expectation in the simplest case (1). From the calculated moments of inertia and vibrational frequencies, we obtained ΔS = 5 kcal mol^{-1} deg^{-1} for this equilibrium. For the hindered pyridine bases, $\Delta S^{\ddagger}$ probably will be somewhat larger. Nevertheless, the apparent activation entropy for the overall process (Scheme I) should be qualitatively similar to that characteristic of a classical S_N2 reaction, as was indeed found experimentally.[5] The relationship of our proposed solution mechanism to the Sneen postulate[17] has been discussed.[2c]

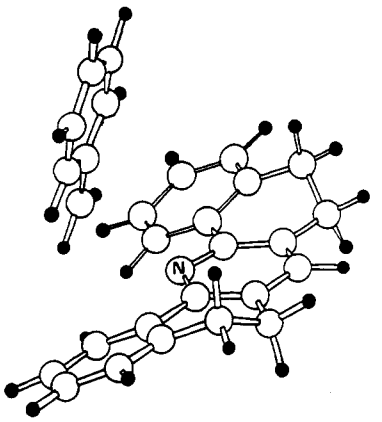

Figure 7. AM1 structure of the ion-molecule complex corresponding to **7**.

Table IV. Heats of Formation of Cations Resulting from Dissociation of *N*-Alkylpyridiniums[a]

cation	AM1	MNDO	PM3	expl
CH_3^+ [b]	252.4	243.9	256.5	261.3[c]
$C_6H_5CH_2^+$ [b]	222.1	218.0	227.4	214.4[d]
4-$CH_3C_6H_4CH_2^+$	209.9	208.5	213.5	
4-$CH_3C_6H_4CH^+Br$	215.8	215.2	225.8	
4-$CH_3C_6H_4CH^+OSi(CH_3)_3$	80.5	68.9	74.2	

[a] Energies in kcal mol^{-1}. [b] Calculated data from ref 10b. [c] Reference 27. [d] Reference 28.

Variation of Calculated Enthalpies with Structure. The overall enthalpies of the starting cation, transition state, ion-molecule complex, and dissociated products (cf. Scheme I and eq 2) as calculated by AM1 are summarized in Table I together with the calculated C-N bond lengths. Less complete data of this type are given for calculations by MNDO (Table II) and for PM3 (Table III). None of these quantities are known experimentally. However, a value of around 107 kcal mol^{-1} may be estimated for the

(17) Sneen, R. A. *Acc. Chem. Res.* **1973**, *6*, 46.

Table V. AM1 Calculated $\Delta\Delta H_f$ Values[a] (kcal mol^{-1})

struct	$\Delta H^{\ddagger}$	$\Delta H'$	ΔH	$\Delta H^{\ddagger} - \Delta H'$	$\Delta H - \Delta H'$	$\Delta H - \Delta H^{\ddagger}$
1	35.3	34.7	44.0	0.6	9.3	8.7
2	33.9	32.7	46.2	1.2	13.5	12.3
3	31.8	26.9	38.1	4.9	11.2	6.3
4	36.6	32.8	45.9	3.8	13.1	9.3
5	34.6	29.9	39.4	4.7	9.5	4.8
6	34.5	25.5	35.4	9.0	9.9	0.9
7	32.0	28.8	41.2	3.2	12.4	9.2
8	29.9	25.2	32.7	4.7	7.5	2.8
9	11.4	2.0	9.0	9.4	7.0	-2.4
10	*b*	*b*	98.3			

[a] For definition of $\Delta H^{\ddagger}$, $\Delta H'$, and ΔH see Figure 1. [b] Energy rises monotonically to dissociated products.

dissociation of **10** using the methods of Drago.[18] This is somewhat larger than the value predicted by AM1 while that for MNDO is still smaller. Alkyl cation affinities are underestimated by the MNDO procedure,[19] due in part to underestimation of stabilization of adjacent positive charge by saturated substituents[19] as well as to the low MNDO predicted heat of formation of the methyl cation (Table IV). Methyl cation affinities also appear to be underestimated at the AM1 level, although the errors of both types are about half those of MNDO.[20] No data of this kind are yet available for PM3.

Unfortunately, it is not possible to estimate benzyl cation affinities in the same way. Here, the errors of the type just mentioned should partially cancel. While the calculated stabilities of pyridinium ions are again expected to be over estimated,[19] so is the heat of formation of the benzyl cation itself (Table IV).

Although the absolute values of the energetic quantities predicted by the semiempirical calculations are uncertain, taken together they form a basis for qualitative discussion. Table V collects the various differences between heats of formation of the species under discussion.

ΔH Values. The ΔH values calculated by AM1 for the benzyl derivatives are 46.2–35.4 kcal mol^{-1}. The three compounds (**3**, **5**, and **6**) with α-*tert*-butyl groups possess the lowest ΔH, suggesting that relief of strain (ca. 8 kcal mol^{-1}) from interaction of the *tert*-butyl/*N*-benzyl groups in the starting compound is released during the dissociation. The conversion of an α-phenyl group to the six-ring fused analogue also reduces ΔH. This effect is quite small while one of the phenyl groups remains free to rotate (e.g., **2** → **4**) but becomes more pronounced in more constrained situations **3** → **6** and **4** → **7** ($\Delta\Delta H$ 2.7 and 4.7 kcal mol^{-1}). The dissociation of **2** is predicted to be to more endothermic than that for **1**. Evidently, the steric strain associated with freely rotating α-phenyl groups is more than offset by their ability to stabilize the pyridinium ion.

$\Delta H'$ Values. Our calculations indicate that an energy minimum exists for each of the compounds corresponding to an ion–molecule complex. The stabilities $\Delta H'$ of the IMC relative to their parent cations lie in an order similar to that for ΔH. However, against this trend, $\Delta H'$ for I–MC **1** is higher than that for I–MC **2**; this again indicates the favorable influence of the α-phenyl groups in the latter. In both these I–MC charge delocalization in the pyridine moiety is unimportant (the charge is localized in the benzyl system, see above). Compared with the pyridine I–MC **1**, the phenyl groups of I–MC **2** increase the polarizability and hence the magnitude of the stabilizing electrostatic attraction. This is reflected in the fact that the phenyl groups of I–MC **2** and the pyridine ring are more nearly coplanar than in the parent cation **2**.

I–MC **2** differ from I–MC **3** by the replacement of a phenyl by a *t*-Bu group, which causes a significant decrease in the $\Delta H'$ value (from 32.7 to 26.9), reflecting the decrease in steric strain of the I–MC comparable to the parent cations.

$\Delta H^{\ddagger}$ Values. These represent the energy barrier formation of the ion–molecule complex. The AM1 method predicts similar activation energies for all the benzyl derivatives, and the variation of $\Delta H^{\ddagger}$ values for the benzyl derivatives is small (viz. over a range of 4.8 kcal mol^{-1} compared to 9.2 kcal mol^{-1} for $\Delta H'$ and 10.8 kcal mol^{-1} for ΔH). The order is changed for $\Delta H^{\ddagger}$ so that the tricyclic compounds (**4–6**) have slightly higher values than either the monocyclic or pentacyclic (**2**, **3**, **7**).

Differences $\Delta H^{\ddagger} - \Delta H'$. These differences represent the energy gained when the transition state collapses into the ion–molecule complex. They represent the increased molecular attraction in the ion–molecule complex as compared to the transition state.

This difference is least for **1**, when little extra energy is gained, and is not much greater in **2**. Compounds **3–5** and **7** show $\Delta H^{\ddagger} - \Delta H'$ value of 3–5 kcal mol^{-1} probably reflecting realignment of the phenyl groups in the ion–molecule complex. The difference is the greatest in the highly strained derivative **6** where considerable reorganization is expected to occur in the ion–molecule complex.

Differences $\Delta H - \Delta H'$. These differences measure the attractive forces between the various pyridines and the benzyl cation. They are least (as expected) in **1**. They are also lower in the *tert*-butyl derivatives than in their phenyl analogues and less in the constrained tricyclic compounds than in their monocyclic analogues.

To evaluate the calculated $\Delta H - \Delta H'$ differences and to estimate the role of competing solvent molecules (see the experimental part below), we chose the benzyl cation together with dichloromethane as a representative system.

The result is that solvent molecules of this polarity can compete only to a small extent with pyridines to form I–MC: relative to the energy of fully dissociated molecules the I–MC $C_6H_5CH_2^+/CH_2Cl_2$ (AM1: ΔH_f = 192.5 kcal mol^{-1}) is stabilized by 3.8 kcal mol^{-1}. This $\Delta H - \Delta H'$ value is significantly smaller than those for I–M complexes of pyridine resulting from the interaction with the same and related cations (7.0–13.5 kcal mol^{-1}, $\Delta H - \Delta H'$ values, Table V.

N–CH_2 Bond Lengths. As summarized in Table I, the N–CH_2 bond lengths r(PyR$^+$) for the *N*-benzyl cations **1–7** do not differ significantly (1.468–1.477 Å). Comparison of the N–CH_2 bond lengths for the C4 phenyl substituted derivatives with the X-ray values[21] shows that the calculated bond lengths are shorter, by 0.022–0.035 Å for **2**, **4**, and **7** and by 0.072 Å for **6**.

For the *t*-Bu substituted I–MC **3**, **5**, and **6** the relatively long (calculated) N–CH_2 bonds r(I–MC) seem to reflect the repulsive (steric) influence of this substituent.

The transition-state N–CH_2 bond lengths are more variable, from 2.28 Å for **1** to 2.08 Å for **6**. The monocyclic and tricyclic series show r(TS) that parallel the corresponding $\Delta H^{\ddagger}$, but the bicyclic series r(TS) are larger than expected.

(18) Kroeger, M. K.; Drago, R. S. *J. Am. Chem. Soc.* **1981**, *103*, 3250.
(19) Ford, G. P.; Scribner, J. D. *J. Comput. Chem.* **1983**, *4*, 594.
(20) The average errors in the MNDO and AM1 methyl cation affinities for the nine amines in Table II in ref 17 are 44.3 and 20.5 kcal mol^{-1}, respectively (the errors fall to 26.9 and 11.6 kcal mol^{-1} if the experimental, rather than the theoretical, heat of formation of CH_3^+ is used), computed from data in ref 19 and this work.
(21) Katritzky, A. R.; Lamba, D.; Spagna, R.; Vaciago, A.; Prewo, R.; Bieri, J. H.; Stezowski, J. J.; Musumarra, G. *J. Chem. Soc. Perkin Trans. 2* **1987**, 1391.

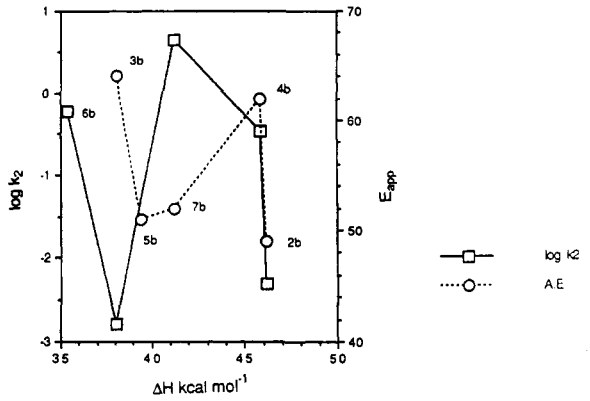

Figure 8. Plots of (a) solution k_2 values (mol^{-1} s^{-1}) for the bimolecular reactions with piperidine in chlorobenzene of compounds **1–10** (**b** derivatives for **2–7**; from ref 28) and (b) appearance potentials (kcal mol^{-1}; from ref 7) against ΔH values.

For cation **9**, the AM1 calculations yield ΔH (9.0 kcal mol^{-1}), $\Delta H'$ (2.0 kcal mol^{-1}), and $\Delta H^{\ddagger}$ (11.4 kcal mol^{-1}) that are significantly below the corresponding values of all of the benzyl derivatives **1–7**. Together with the $\Delta H^{\ddagger} - \Delta H'$ of 9.4 kcal mol^{-1} these data predict that dissociation as in Scheme I via the corresponding I–MC **9** should be facile. This can be interpreted as the result of the stabilizing influence of a oxygen lone pair, which is more pronounced in the I–MC **9** and in the corresponding (substituted) benzyl cation than in the parent cation.

Comparisons with Experimental Data. As summarized in Figure 2, the AM1 results for ions **1**, **5**, **8**, and **9** give a clear order for the heat of activation $\Delta H^{\ddagger}$ and therefore for the first step in an S_N1 reaction. Furthermore, a large heat of dissociation is predicted for **10** from which methyl-group transfer is indeed very difficult.[22] The ease of such dissociations for the other compounds seems to follow the above order, which within the monocyclic and within the tricyclic series parallels that for $\Delta H'$ (the values for the pentacyclic compounds are increased compared to those for the monocyclic derivatives). These relationships are discussed further in our previous communications.[23,24]

Precise comparisons with experimental results in chloroform solution are difficult, although many *N*-alkylpyridinium cations can undergo N^+–alkyl bond scission in chlorobenzene in first-order reactions at rates that can be measured for *N*-(secondary alkyl)pyridiniums. But they are usually too slow to measure for the *N*-benzyl derivatives.[2]

Although the bromo substituent in **8** is predicted to reduce the $\Delta H^{\ddagger}$ value for dissociation, this compound undergoes preferential substitution of bromide under experimental conditions that are much milder (CH_2Cl_2, 20 °C) than those applied to the salts **2–7** (100 °C, chlorobenzene).[23a-c]

Experimental rates for the transfer of *N*-benzyl to the piperidine in chlorobenzene solution at 100 °C have been recorded for a wide range of *N*-benzylpyridinium cations.[2] This work has shown the rate of transfer to be in the order **1** < **2** < **4** < **7** with **6** being toward the faster end of this range, which is in fair agreement with the order reported above for $\Delta H'$.

However, there is no quantitative relation between ΔH, $\Delta H'$, or $\Delta H^{\ddagger}$ values (or any of their differences) and the solution k_2 value for the bimolecular reactions of these compounds with piperidine in chlorobenzene solution[25] (see, e.g., Figure 8). Further, the gas-phase appearance potentials for the heterolysis of the C–N bonds in these compounds are not related directly to any of these quantities.[26]

All methods predict that the ion **9** should show the lowest barrier to S_N1 dissociation. This agrees with the recently found behavior of **9** toward neutral (and negatively charged) nucleophiles as a powerful (trimethylsilyl)oxy–alkyl group transfer reagent, in which the unsubstituted pyridine moiety serves as a neutral leaving group.[23a,24] These relationships are discussed further in our previous papers.[23,24]

Acknowledgment. A.R.K. and E.A. are indebted to the NATO committees of their countries (USA and Germany) for financial support. E.A. gratefully ackowledges support by the "Deutsche Forschungsgemeinschaft" and the "Fonds der Chemischen Industrie". G.P.F. is grateful to the National Institutes of Health for partial support for this work through Grant No. CA 30475. J.G.T. thanks the Universitaet Erlangen-Nuernberg and the "Studienstiftung des deutschen Volkes" for a scholarship. The Harris H800 minicomputer on which some of the calculations were performed (at SMU) was a gift from the Harris Corp.

(22) Katritzky, A. R.; Benerji, A.; El-Osta, B. S.; Parker, I. R. *J. Chem. Soc., Perkin Trans. 2* **1979**, 690.

(23) (a) Anders, E.; Markus, F.; Meske, H.; Tropsch, J. G.; Maas, G. *Chem. Ber.* **1987**, *120*, 735. Anders, E.; Tropsch, J. G. *Bull. Soc. Chim. Belg.* **1987**, *96*, 719. (b) Anders, E.; Tropsch, J. G.; Katritzky, A. R.; Rasala, D.; Vanden-Eynde, J.-J. *J. Org. Chem.* **1989**, *54*, 4808. (c) Maquestiau, A.; Anders, E.; Vanden-Eynde, J.-J.; D'Oranzio, P.; Mayence, A. *Bull. Soc. Chim. Belg.* **1989**, *98*, 523.

(24) Anders, E.; Hertlein, K.; Meske, H. *Synthesis* **1990**, 323. See also: Hertlein, K. Diplomarbeit, University of Erlangen, 1988.

(25) Katritzky, A. R.; Musumarra, G.; Sakizadeh, K. *Tetrahedron Lett.* **1980**, 2701.

(26) Katritzky, A. R.; Malhotra, N.; Savage, G. P.; Eyler, J. R.; Watson, C. H.; Zimmerman, J. A. Unpublished results.

(27) Traeger, J. C.; McLoughlin, R. G. *J. Am. Chem. Soc.* **1981**, *103*, 3647.

(28) Baer, T.; Morrow, J. C.; Shao, J. D.; Olesik, S. *J. Am. Chem. Soc.* **1988**, *110*, 5633.